NF

NASA Technical Memorandum 82612

A Theoretical Approach to Sound Propagation and Radiation for Ducts with Suppressors

Edward J. Rice
Lewis Research Center
Cleveland, Ohio

and

David T. Sawdy
Boeing Military Airplane Company
Wichita, Kansas

Prepared for the
One-hundred-first Meeting of the Acoustical Society of America
Ottawa, Ontario, Canada, May 18-22, 1981

A THEORETICAL APPROACH TO SOUND PROPAGATION AND RADIATION FOR DUCTS WITH SUPPRESSORS

by Edward J. Rice

National Aeronautics and Space Administration

Lewis Research Center

Cleveland, Ohio 44135

and

David T. Sawdy

Boeing Military Airplane Company

Wichita, Kansas 67221

ABSTRACT

The several phenomena involved in theoretical prediction of the far-field sound radiation attentuation from an acoustically lined duct have been studied. These include absorption by the suppressor, termination reflections, and far-field radiation. Extensive parametric studies have shown that the suppressor absorption performance can be correlated with mode cut-off ratio or angle of propagation. The other phenomena can be shown to depend explicitly upon mode cut-off ratio. A complete system can thus be generated which can be used to evaluate aircraft sound suppressors and which can be related to the sound source through the cut-off ratio-acoustic power distribution. Although the method is most fully developed for inlet suppressors, several aft radiated noise phenomena will also be discussed. This paper summarizes this simplified suppressor design and evaluation method, presents the recent improvements in the technique and discusses areas where further refinement is necessary. Noise suppressor data from engine experiments are compared with the theoretical calculations.

E-863

INTRODUCTION

The ultimate goal of noise suppressor research, as applied to aircraft applications, is to develop the ability to predict sound attenuation in the far-field as a function of directivity angle. It is desirable to perform this modeling with a purely theoretical foundation so that it will be of general application and not tied to specific configurations or operating conditions as would be the case if an empirical foundation were used. This suppressor modeling should be applicable to all aircraft operating conditions from static testing to actual flight. This goal is extremely demanding since it requires the integration of all aspects of acoustics research including noise source modeling, sound propagation in acoustically treated ducts, scattering by flow gradients and duct discontinuities (such as wall impedance or the duct termination), and radiation to the far-field through a flow field which varies from a high Mach number in the duct to a lower Mach number (or zero flow) in the far-field. Analytical solutions do not exist for some aspects of this problem so that conventional modal analysis cannot be carried through from the source to the far-field. Obviously approximate methods must be used to fill the voids where they exist.

This paper presents a simplified modeling procedure based upon mode cut-off ratio which shows promise in handling this extremely complex problem. It should be emphasized that the cut-off ratio method is not an analysis technique in itself but rather a means of interpreting the results of separate exact analyses where they exist. This method, in its interpretation of results, is closely allied to geometric acoustics so that ray methods can be used where other analysis does not exist.

There have been numerous contributions to the analysis of sound propagation in acoustically lined ducts upon which some of the elements of this

paper are built. However, no attempt will be made to review all this work, but rather only those contributions directly related to the cut-off ratio method. Surveys of the duct acoustics literature have been presented by Nayfeh, et al.,[1] Vaidya and Dean,[2] and Syed and Bennett.[3] Not all of the physics of suppressor sound propagation have been incorporated into the cut-off ratio method at this time as will become evident in later discussions.

The key discovery which has led to the cut-off ratio method of suppressor analysis was made by Rice[4] who demonstrated that the optimum wall impedance and maximum possible attenuation for single modes propagating within a suppressor, with a uniform steady flow with wall boundary layers, could be approximately correlated with mode cut-off ratio. This was significant in that it implied that individual modal identity was not required and that modes with similar cut-off ratios would behave similarly within an inlet duct suppressor. Rice[5] proposed the cut-off ratio method as a suppressor design method and proceeded to develop the tools needed to handle the entire sound propagation problem including a modal density function,[6] the duct termination loss,[7] and the far-field radiation pattern.[7] All elements of the method require modal information only in terms of mode cut-off ratio with the actual modal identification being suppressed. Anderson (unpublished presentation at the 96th Meeting of the Acoustical Society of America, Honolulu, Hawaii, Dec. 1978) has correctly pointed out that for a single mode incident upon a suppressor from a hardwalled duct, modal information is necessary to determine the suppressor optimum impedance characteristics. However, this solution introduces the complicating factor of modal scattering which obscures the simplicity of the cut-off ratio method. In actual use[8] it is assumed that when many modes are present the modal

scattering balances out among the various cut-off ratio regimes. Modal scattering must be studied further and incorporated into the present method.

The calculation of far-field radiation patterns has been studied for several years. Tyler and Sofrin[9] presented the radiation pattern for a flanged duct. The Wiener-Hopf technique has been used to analyze the radiation from an unflanged circular duct by Levine and Schwinger,[10] Carrier,[11] Weinstein,[12] Lansing,[13,14] Homicz and Lordi,[15] and Savkar.[16,17] Munt[18] and Rienstra[19] have included the shear layer instability required for low frequency propagation from an exhaust duct. Candel[20] and Koch[21] have studied radiation from unflanged two dimensional ducts. Far-field radiation has been studied using spherical wave functions by Mungur, et al.,[22,23] Plumblee,[24] Whitesides and Mungur,[25] Beckemeyer, et al.,[26] and Sawdy, et al..[27] These latter studies allow the matching of conical ducts to the far-field. All of these radiation models suffer a common weakness. They cannot describe the radiation from an aircraft inlet under general operating conditions. At static test conditions the inlet has a large Mach number flow within the duct but there is no flow in the far field. The inflow follows approximately radial streamlines into the inlet. In flight the inlet captures a streamtube whose diameter depends upon the flight speed and the velocity inside and outside of this tube is the same (relative to the inlet). The flanged duct radiation model is formulated for zero flow inside and outside the duct. The Wiener-Hopf technique can handle two separate parallel flows which is an excellent model for exhaust radiation but it models inlet radiation only when the flight Mach number equals the duct Mach number. A later discussion will suggest a way of using this unflanged duct solution for inlets by removing the unwanted refraction effects due to the slip layer. In this paper a modified

form of the flanged duct solution will be used. This solution is simple and can be approximated by an expression which contains the modal information only in the form of cut-off ratio.[7] This is a key requirement for coupling the radiation solution to the duct solution and the source condition. Also simple transformations can be applied to handle the effects due to differences between duct flow and exterior Mach numbers.[28,29] These simple angle transformations have been used by Rice and Saule[30] to show that convection and refraction effects can be added to the flanged duct solution so that it very accurately approximates the more exact Wiener-Hopf solution which is valid for aft radiation.

The duct reflection coefficient and termination loss are inherent in the Wiener-Hopf radiation solution. However, as discussed above this method is inadequate for aircraft inlets as well as being too complex for routine calculations. Zorumski[31] has studied the termination effects for the flanged duct case. A simple approximate equation[7] dependent only on cut-off ratio has been derived from his results.

The final consideration involves the description of the noise source. Single mode assumptions (usually least attenuated mode) have been used by Motsinger, et al.[32] and Minner and Rice[33] for thin rectangular ducts which might approximate the annular passages of an inlet or aft duct with splitter-rings. This assumption has provided good results for these heavily suppressed inlets and aft fan ducts but it is not valid for engine inlets with wall suppression only.[34] The assumption of equal acoustic power per mode has been used by Ko[35] in theory-data comparisons for a flow-duct and by Syed and Bennett[3] for engine tests. Rice and Heidelberg[8] used equal power per mode in the first attempt to predict far-field radiation attenuation using the cut-off ratio technique. The technique incorporated a bias-

ing function which could be used to alter the modal distribution away from equal power, but since a no-flow radiation function was used in the theory it was not believed worthwhile to use the biasing function. In this paper an improved method for estimating the source power distribution will be introduced.

The viable alternatives to the method presented here for predicting radiation attenuation for an aircraft inlet are very limited. Purely numerical techniques show great promise but will require extensive development which is in progress. Numerical approaches will not be considered in this paper. Baumeister[36] has recently presented a review of the progress in numerical analysis in acoustics. Classical modal analysis, although containing the modal scattering presently missing from the present approach, cannot currently be carried to the far-field through the complex flow field present near the inlet lip. Syed and Bennett[3] have predicted power attenuation but had to resort to a purely empirical fit of the directivity attenuation. They also had to restrict the number of modes used (selected representative modes) to keep their computer time within reasonable bounds. Kempton[37,38] has presented a geometric acoustics approach to predict far-field radiation attenuation for straight, converging, and diverging inlets. His results for straight inlets are qualitatively very similar to the results of the cut-off ratio method presented here. His comparison of ray acoustics results with no-flow modal predictions were quite good. Rice[39] has also shown good correspondence between the ray method and modal analysis within acoustically lined ducts. Ray tracing in suppressors deviates from modal analysis in the limits of either grazing or nearly normal incidence. Unfortunately, Kempton's technique has been developed so far only for no-flow in the duct. Perhaps an extension of his method, using the ray tracing

method of Cho and Rice[40] through velocity gradients, may provide a powerful analysis method for radiation from aircraft inlets with suppressors.

SYMBOLS

A_i	coefficients in the modal biasing function, see Eq. (29)
B_s	amplitude of discrete mode, see Eq. (27)
B3	acoustic liner configuration reported in Ref. 49
C_g	group velocity vector, m/sec
C_p	phase velocity vector normal to wave front, m/sec
c	speed of sound, m/sec
D	duct diameter, m
$\mathscr{D}(\xi_D)$	modal density function, see Eq. (28)
$\Delta dB(\psi)$	far-field radiation directivity attenuation, see Eq. (32), dB
$\Delta dB(\xi_D)$	suppressor attenuation as a function of mode cut-off ratio, dB
ΔdB_m	maximum possible attenuation for a mode at its optimum impedance, dB
$F(\xi_D)$	modal biasing function, see Eq. (29)
f	frequency, Hz
$G(\psi_o,\xi_o)$	correction factor for flanged duct radiation equation, see Eqs. (17) and (22)
$H(\psi_D,\xi_D)$	Multiplying factor in far-field radiation equation of inlet when transforming from no-flow to uniform flow conditions
k	ω/c, m^{-1}
L	duct length, m
M_D	duct flow Mach number
M_∞	flow Mach number in far-field
m	spinning mode lobe number (circumferential order)

P_E	far-field acoustic pressure for single modes with equal acoustic power, see Eq. (24), N/m^2
P_{EX}	experimental far-field acoustic pressure, N/m^2
P_m	multimodal far-field acoustic pressure for hardwalled inlets, see Eq. (27), N/m^2
P_{ma}	multimodal far-field acoustic pressure for softwalled inlet, see Eq. (31), N/m^2
$Q(\xi_D)$	function of cut-off ratio, see Eqs. (24) and (25)
R	inlet termination reflection coefficient, see Eq. (21)
r	radial coordinate, m
r_o	circular duct radius, m
T	inlet termination transmission loss, see Eq. (19)
α	hardwall duct eigenvalue or magnitude of complex softwalled duct eigenvalue
β	$\sqrt{1 - M_D^2}$
δ	boundary layer thickness (1/7th power law), m
ϵ	normalized boundary layer thickness, δ/r_o
η	frequency parameter, fD/C
θ	specific acoustic resistance of acoustic liner
ξ_D	mode cut-off ratio with duct flow, see Eq. (1)
ξ_{DS}	mode cut-off ratio in softwalled duct with flow, see Eq. (5)
ξ_o	mode cut-off ratio zero duct flow
ξ_S	mode cut-off ratio of single descrete mode
ρ	density of air, kg/m^3
τ	$\sqrt{1 - 1/\xi_D^2}$
τ_o	$\sqrt{1 - 1/\xi_o^2}$
ϕ	phase of complex eigenvalue for softwalled duct, deg

ϕ_r phase velocity propagation angle relative to radial coordinate, angle of incidence on wall, deg

ϕ_x phase velocity propagation angle relative to axial coordinate, deg

X specific acoustic reactance of acoustic liner

ψ far-field angle measured from inlet axis, deg

ψ_D angle between group velocity vector and duct axis with flow in inlet duct, deg

ψ_o ψ when no duct flow considered, deg

ψ_p ψ for principle lobe peak, see Eq. (23), deg

ψ_x angle between group velocity vector and duct axis in general case, deg

ω circular frequency, rad/sec

SIMPLIFIED APPROXIMATE SUPPRESSOR THEORY

In this section the elements of the simplified suppressor theory will be outlined. The emphasis will be placed upon the concepts involved, and most of the mathematical expressions upon wnich the technique is based will be referenced for the reader who wishes to pursue them further. Only those equations which are deemed necessary for clarity or which are modifications to previously published results will be presented. Since the mode cut-off ratio is the key to the method some discussion of it will first be presented.

Cut-off Ratio and Angles of Propagation

The relationships between the mode cut-off ratio and the angles of propagation are useful in visualizing the physics of the sound propagation and help in the understanding of why a suppressor theory based upon cut-off ratio should work. The modal cut-off ratio with a steady flow Mach number (M_D) in the hard walled duct is defined as

$$\xi_D = \frac{kr_o}{\alpha\sqrt{1 - M_D^2}} = \frac{\pi n}{\alpha\sqrt{1 - M_D^2}} \tag{1}$$

which is consistent with the derivation of Sofrin and McCann.[41] For $\xi_D > 1$ the mode propagates, for $\xi_D < 1$ the amplitude of the mode decays exponentially with axial distance.

In Fig. 1 the propagation vectors and angles of propagation are shown. The phase velocity vector, C_p, is normal to the wave front. The steady flow axial velocity (cM_D) is subtracted (for inlet flow) from C_p to yield the group velocity vector C_g. The angles of propagation are given by[28,29]

$$\cos\phi_x = \frac{-M_D + \sqrt{1 - 1/\xi_D^2}}{1 - M_D\sqrt{1 - 1/\xi_D^2}} \tag{2}$$

$$\cos\psi_x = \frac{M_D + \cos\phi_x}{\sqrt{1 - M_D^2 + 2M_D\cos\phi_x}} \tag{3}$$

and at $r = r_o$

$$\cos\phi_r\Big]_{r_o} = \frac{\sqrt{1 - M_D^2}\ \sqrt{1 - (m/\alpha)^2}}{\xi_D\left(1 - M_D\sqrt{1 - 1/\xi_D^2}\right)} \tag{4}$$

which represents the angle of incidence upon the wall. From Eqs. (1) and (2) it can be seen that as $\xi_D \to \infty$ both ϕ_x and $\psi_x \to 0$, that is both the phase and group velocities are axial and thus the propagation is purely axial. When $\xi_D \to 1$, $\cos\phi_x \to -M_D$ and $\psi_x \to 90°$, or the group velocity, which is associated with acoustic power flux, is purely

transverse. It has been shown[28] that when the flow Mach number outside of the duct (in the far-field) is the same as in the duct, the peak of the principal lobe of radiation also occurs at ψ_x. When there is no flow in the far-field but flow in the duct, the far-field radiation peaks at ϕ_x. An interesting example can be shown at $\xi_D = 1$ and thus $\cos \phi_x = -M_D$. If $M_D = -0.4$, $\phi_x = 66.4°$. Thus near mode cut-off, for a static engine test, radiation would peak at about 66° from the inlet axis rather than at 90° as often perceived.

Inspection of Eq. (4) shows that for modes with m/α small, the angle of incidence on the duct wall has modal information only in the form of cut-off ratio. It is known that absorption of sound by a suppressor depends upon the angle of incidence and thus is dependent upon the cut-off ratio.

Suppressor Performance

The sound attenuation in a cylindrical suppressor is obtained by using correlations of the optimum impedance and maximum possible attenuation. These feed into a correlation of the actual damping contours which are approximated as circles and used to estimate off-optimum suppressor performance.

The concepts of optimum impedance and maximum possible attenuation are illustrated in Fig. 2. Equal damping contours representing exact calculations for a particular mode ($m = 7$, $\mu = 1$) are represented by the solid lines. As damping is increased, the contours shrink in size and the limit is represented by the optimum impedance. The damping at this limiting impedance is called the maximum possible attenuation for this mode. Pushing to higher attenuations would result in a contour which can be related to the next higher radial mode ($\mu = 2$ in this case). Rice[4] discovered that these optimum impedances could be approximately correlated with mode cut-off ratio defined in the soft-walled duct as

$$\xi_{DS} = \frac{\pi n}{\alpha \sqrt{\left(1 - M_D^2\right) \cos 2\phi}} \tag{5}$$

This led to the important simplification in suppressor theory that individual modes need not be considered. All modes with similar cut-off ratios will behave similarly in a lined duct. Rice[42] pursued this approach with a wide range parametric study of optimum impedance which resulted in simple correlating equations for both optimum resistance and reactance. An example is shown in Fig. 3. The symbols represent samples of all of the modes while the curves represent the results of the correlating equations. It is seen that for fixed Mach number, frequency parameter, and boundary layer thickness, all of the modes lie along a common curve. It is interesting to note that the optimum resistance is a strong function of boundary layer thickness for high cut-off ratios (mainly axial propagation) but is independent of cut-off ratio nearer to cut-off (mainly transverse propagation). This is reasonable since for transverse propagation the wave vector is mainly parallel to the direction of the velocity gradient of the boundary layer.

Note that in Eq. (5) the cut-off ratio definition differs from that in a hard-walled duct (Eq. (1)). This is due to the complex eigenvalue with phase ϕ encountered in the suppressor. It should also be pointed out that for the lowest radial orders of a high lobed (large m) mode, the optimum impedance deviates somewhat from the correlation of Ref. 42. This can be understood from the inspection of Eq. (4). When m/α is not much less than unity, as for the modes mentioned above, the angle of incidence is a weak function of mode information as well as cut-off ratio. Rice[39] has shown that angle of incidence is perhaps a more basic parameter than cut-off ratio in suppressor performance. However, cut-off ratio is more convenient and

small errors in a few modes when many are present are not serious. It should be cautioned that for single mode calculations some error may occur and it is sometimes these high m, low radial order modes that occur at discrete tones in actual engines.

The maximum possible attenuation was also shown to be approximately correlated by cut-off ratio alone.[5] The expression used here is

$$\frac{\Delta dB_m}{L/D} \approx \frac{327\ \xi_D}{\sqrt{1 - M_D^2}} \left\{ \frac{0.9221}{\xi_D^2} - 1 + \sqrt{1 - \frac{1.8442}{\xi_D^2} + \frac{0.879}{\xi_D^4}} \right\}^{1/2} \qquad (6)$$

Equation (6) shows that maximum possible attenuation is a function only of cut-off ratio, Mach number and duct L/D. Although optimum impedance can be a strong function of boundary layer thickness,[42,43] it was shown in Ref. 43 that the maximum damping is insensitive to boundary layer thickness.

Algebraic equations are thus available for both the optimum impedance and the maximum attenuation at this impedance which are functions of duct Mach number, boundary layer thickness, frequency parameter, and cut-off ratio. However, seldom is the actual wall impedance coincident with this optimum. To handle off optimum impedances an equation was developed for circular constant attenuation contours which closely approximate the actual attenuation contours. An example of the results of this equation is shown in Fig. 2. The contour equation was first developed from an extensive study of well propagating modes[44] (large ξ_D) and then modified[8] to handle near cut-off modes ($\xi_D \approx 1$) and boundary layers.

The use of the suppressor attenuation package can be summarized as follows. It is assumed that duct geometry, flow, boundary layer thickness, frequency, and liner impedance are known. A cut-off ratio is chosen which then allows calculation of the optimum impedance and maximum possible

attenuation. These are then used in the circular contour equation (along with M_D, η and the wall impedance) to calculate the actual attenuation for the liner. This is repeated for a series of cut-off ratios to determine $\Delta dB(\xi_D)$ as a function of ξ_D.

FAR-FIELD RADIATION AND DUCT TERMINATION LOSS

In order to make full use of the simplified cut-off ratio method in the acoustic liner, a far-field radiation expression must be developed which contains all the modal information in the form of cut-off ratio. Out of necessity, the expression used had to be simple in form, which eliminates the Wiener-Hopf and spherical wave function methods. The starting point is thus the zero flow flanged duct radiation expression of Tyler and Sofrin.[9] Saule[45] presented a modified form of this equation which yields equal acoustic power per mode

$$P^2 = \frac{(\pi\eta)^3 \sqrt{(\pi\eta)^2 - \alpha^2}\, \sin^2\psi_0 [J_m'(\pi\eta \sin\psi_0)]^2}{[1 - (m/\alpha)^2]\left[\alpha^2 - (\pi\eta \sin\psi_0)^2\right]^2} \tag{7}$$

Rice[7] further modified this equation to suppress modal information except in the form of cut-off ratio to obtain

$$P^2 \approx \frac{2 \sin\psi_0 \sqrt{1 - 1/\xi_0^2}\left\{\sin[\pi\eta(\sin\psi_0 - 1/\xi_0)]\right\}^2}{\pi^2\eta\left[1/\xi_0^2 - \sin^2\psi_0\right]^2} \tag{8}$$

where the sinusoidal approximation for the Bessel function was used and it was assumed that $m/\alpha << 1$. The zero subscripts are used in Eqs. (7) and (8) to denote zero Mach number. Equation (8) has been compared to Eq. (7) by Saule and Rice[46] for several modes. This approximation was found to be more adequate than expected with only minor error except for the lower

radial, high lobe number (large m) modes which violate both of the above assumptions. Equation (8) has been used[7,46] extensively to generate approximate multimodal radiation patterns using an extremely simplified integration (over ξ_o) scheme. These multimodal radiation directivities fit more exact calculations very accurately.[7,46]

Rice, et al.[28] extended the work of Candel,[20] Lansing, et al.,[14] and Homicz and Lordi[15] (whose radiation expressions are valid either for no flow or for interior and exterior flows equal) to handle the case of radiation from a duct with an axial flow Mach number (M_D) to an ambient field with axial Mach number (M_∞). An important special case of this is the static engine test where $M_\infty = 0$ which will be reviewed here. The concepts behind the angle transformations which will be given below can be shown by a discussion of Fig. 1. The phase velocity vector, C_p, is normal to the wave front and propagates at an axial angle ϕ_x. Note that for a given mode (eigenvalue α) at a given frequency (η) the cut-off ratio is a function of duct Mach number, M_D, as seen from Eq. (1). Equation (2) shows that ϕ_x is further modified by duct Mach number (M_D) and thus the wave front for a given mode propagates at a different angle with duct flow than for no-flow. An additional effect of duct flow is that the duct flow velocity (cM_D) must be subtracted (for an inlet case) from the phase velocity vector (C_p) to form the group velocity vector (C_g). The acoustic power propagates in the direction of C_g. It has been shown[28] that if the far-field Mach number is the same as the duct Mach number the bulk of the acoustic power will be radiated at angle ψ_x. Diffraction at the inlet lip will occur to form sidelobes, but the peak of the principal lobe of radiation will occur at ψ_x. The more interesting case, for which no exact solution is available for an inlet flow, is when the exterior Mach

number is different than the duct Mach number. If the exterior Mach number is zero, as in a static test case, the axial flow velocity vector must be removed and the sound will propagate normal to the wave front at angle ϕ_x. Only refraction, reflection off a bellmouth, or altering M_D and ξ_D by a geometry change can change ϕ_x (see Ref. 40 for a discussion of the refraction effect). The change in ϕ_x due to sound passing through a gradual geometry variation can be deduced from the work of Cho[47] and the alteration of the radiation directivity for the no-flow case has been demonstrated by Posey, et al.[48] For the results presented here no alteration of ϕ_x by the above effects is considered. These effects, still in the research stage, can be added later.

The above discussion, although focusing on the static engine test case, is far more general than at first appears. In flight the wave front is always discharged into a static environment and thus it is propagating at angle ϕ_x. Retarded time effects accounting for the travel time of the wave from the aircraft to the observer will alter the apparent radiation directivity and must be considered. Only for wind tunnel tests or for microphones mounted on the aircraft must an external Mach number other than zero be considered.[28]

The angle transformations just discussed will now be presented. To convert from zero Mach number everywhere (in-duct and far-field) to uniform Mach number (M_D) everywhere the following substitutions are used.[14,15,20] Replace $\sin \psi_0$ by

$$\sin \bar{\psi} = \frac{\beta \sin \psi_D}{\sqrt{1 - M_D^2 \sin^2 \psi_D}} \tag{9}$$

$\cos \psi_0$ by

$$\cos \bar{\psi} = \frac{\cos \psi_D}{\sqrt{1 - M_D^2 \sin^2 \psi_D}} \tag{10}$$

η by

$$\bar{\eta} = \frac{\eta}{\beta} \tag{11}$$

and ξ_0 by

$$\bar{\xi} = \frac{\xi_D}{\beta} \tag{12}$$

where

$$\beta = \sqrt{1 - M_D^2} \tag{13}$$

The term ψ_D denotes the angle from the inlet axis for the case where a Mach number M_D exists inside the duct and in the far-field.

Equations (7) or (8) must also be multiplied by,

$$H(\psi_D, \xi_D) = \frac{1 - M_D \cos \psi_D}{1 - M_D \sqrt{1 - 1/\xi_D^2}} \tag{14}$$

for the inlet case.[14,15,20] For exhaust radiation the factor $H = 1$.

The removal of the far-field Mach number (thus $M_\infty = 0$) was first developed[28] for principal lobe radiation and then generalized[29] for any arbitrary angle. This transformation which replaces ψ_D by the final far-field radiation angle ψ is given by

$$\cos \psi_D = \frac{M_D + \cos \psi}{\sqrt{1 + M_D^2 + 2M_D \cos \psi}} \tag{15}$$

or

$$\cos \psi = -M_D \sin^2\psi_D + \cos \psi_D \sqrt{1 - M_D^2 \sin^2\psi_D} \qquad (16)$$

Before these angle transformations are made in Eq. (8) two other extensions of the radiation theory must be considered: an approximate unflanged duct correction and maintenance of equal energy per mode in the two flow Mach number system.

Approximate Unflanged Duct Correction Factor

Since the radiation pattern is shifted toward the inlet axis when a duct Mach number is present with no-flow in the far-field, the flange position (90°) is shifted into the front quadrant and errors will be encountered at angles beyond $\psi = 66°$ for $M_D = -0.4$. A correction factor was thus needed to make the flanged duct radiation directivity more closely resemble the unflanged duct directivity which is valid for all angles.

Sawdy ("Cutoff Ratio Analysis for Predicting Inlet Liner Suppression Performance," Boeing Document No. D3-11719-1, unpublished) has extended the work of Levine and Schwinger[10] to derive an unflanged duct correction factor for use with either Eq. (7) or (8) which is valid for a general mode and for the no-flow case. This factor is expressed as

$$G(\psi_0, \xi_0) = \frac{(\cos \psi_0 + \tau_0)^2 + 2R\left(1/\xi_0^2 - \sin^2\psi_0\right) + R^2(\cos \psi_0 - \tau_0)^2}{1 - R^2} \qquad (17)$$

where

$$\tau_0 = \sqrt{1 - 1/\xi_0^2} \qquad (18)$$

and R is the termination reflection coefficient. The reflection coefficient can be evaluated by using an approximate termination transmission loss developed by Rice[7]

$$T(\xi_0) \approx \frac{4\tau_0}{(1 + \tau_0)^2} \tag{19}$$

which was shown to approximate the results of Zorumski.[31] The reflection coefficient is determined from

$$R^2(\xi_0) = 1 - T(\xi_0) \tag{20}$$

or

$$R(\xi_0) = \frac{\tau_0 - 1}{\tau_0 + 1} \tag{21}$$

Using Eqs. (18) and (21) in (17) reduces Sawdy's expression to,

$$G(\psi_0,\xi_0) \approx \tau_0(1 + \cos\ \psi_0)^2 \tag{22}$$

It is interesting to note that the angle dependence of $G(\psi_0,\xi_0)$ is exactly the same as the Kirchoff approximation discussed by Weinstein[12] and Levine and Schwinger.[10]

Recall that Eq. (22) will be used as a multiplier of either Eq. (7) or (8) to better approximate the unflanged duct radiation pattern. Notice that between $\psi_0 = 0$ and $\psi_0 = 90^\circ$, $G(\psi_0,\xi_0)$ is reduced by a factor of four (or -6 dB) which is precisely what is needed to remove the pressure doubling of the reflection at the flange.

Final Radiation Equation for Equal Acoustic Power per Mode

Recall that Eq. (8) was an approximate radiation expression developed for a flanged duct with no-flow and equal acoustic power per mode. We are in the process of deriving an approximate unflanged duct radiation expression which is valid with flow in the duct but no-flow in the far-field. Since no exact solution has been shown to exist for this problem several

kinematic arguments have been utilized to derive an expression. There is no reason to believe that the final expression would provide the desired equal acoustic power per mode solution in the far-field. A coefficient must be derived which will guarantee this equal acoustic power distribution.

Rice and Saule[30] have shown, using Eq. (8), that the product of the acoustic pressure amplitude of the principal lobe peak (principal lobe contains most of power) and the solid angle subtended by the principal lobe (on a constant radius sphere) is a constant. The acoustic pressure in a principal lobe thus falls off as the mode is shifted toward the sideline because the solid angle increases and acoustic power must be maintained. They used this simple principle obtaining excellent results in an aft radiation study. This same method will be used here to obtain a normalizing factor.

The principal lobe peak has been shown[28] to be located at

$$\sin \psi_p = \frac{\beta}{\xi_D \left[1 - M_D \sqrt{1 - 1/\xi_D^2}\right]} \tag{23}$$

If Eq. (8) is multiplied by Eq. (22), then the transformations of Eqs. (9) to (12) applied, the result multiplied by Eq. (14), and finally the transformation of Eq. (15) applied, then the un-normalized radiation expression will be obtained. This intermediate result will not be given here. Requiring that the product of the acoustic pressure amplitude of the principal lobe peak and the subtended area of this lobe be a constant, results in the final equation,

$$P_E^2(\psi,\xi_D) \approx Q(\xi_D)\left(\frac{\sin\psi}{1+M_D\sin\psi}\right)\left(1+\frac{M_D+\cos\psi}{1+M_D\cos\psi}\right)^2\left[1-\frac{M_D(M_D+\cos\psi)}{\sqrt{1+M_D^2+2M_D\cos\psi}}\right]^2$$

$$\times\frac{\sin^2\left[\pi n\left(\frac{\sin\psi}{1+M_D\cos\psi}-\frac{1}{\beta\xi_D}\right)\right]}{\left[\frac{1}{\beta^2\xi_D^2}-\frac{\sin^2\psi}{(1+M_D\cos\psi)^2}\right]^2} \qquad (24)$$

where,

$$Q(\xi_D) = \frac{2\tau(1+M_D\tau)(1-M_D\tau)^3}{\pi^2\eta\beta^4(1+\tau)^2\left[\sqrt{1-M_D^2\tau^2}-\beta M_D\tau\right]^2} \qquad (25)$$

$$\tau = \sqrt{1-1/\xi_D^2} \qquad (26)$$

Equation (24) has been integrated numerically over the principal lobe for several values of ξ_D and found to contain almost equal acoustic power for all cases.

Although Eq. (24) is quite lengthy, it is a closed form algebraic equation which describes the inlet radiation for the complicated but realistic case of flow in the duct but no flow in the far-field. This expression is the only one known to the authors which attempts to describe this complex phenomenon.

Before examining results of calculations using the inlet radiation equation, the case of aft radiation with flow will be reviewed. This case provides some confidence in the angle transformations for a problem for which an exact solution exists.

Simplified Aft Radiation Model

The aft duct of an engine can be simulated by a cylindrical jet discharging into a static surrounding medium with a slip layer separating the two regions. This problem can be solved exactly using the Wiener-Hopf technique which has been done by Savkar[16,17] whose program will be used here to generate the exact results. Rice and Saule[30] have also solved this radiation problem starting with the zero flow flanged duct radiation relation (Eq. (8)). The same angle transformations were used as in the previous sections, but with the addition that the refraction effect through the shear layer was considered. The exact and approximate radiation directivities are compared in Fig. 4 (from Ref. 30). The agreement is surprisingly good. The location of the peaks and valleys are well described. The location of the zone of silence is also well represented. Small errors occur in the magnitudes of the side lobes which are probably due to solid angle changes caused by shifts in location which could be corrected for if deemed necessary. The conclusion from this comparison is that convection, refraction, and diffraction effects can be handled by the simple procedures used in this paper.

One major difference occurs between inlet and aft radiation which is relevant to the use of the flanged duct radiation equation as a starting point in the analysis. Recall that beyond $\psi_0 = 90^\circ$, the flange duct radiation equation is not valid even with the correction factor of Eq. (22). This is because sidelobes occur in the rear quadrant and the Wiener-Hopf method shows that these cannot occur.[15] For aft radiation with duct flow this $\psi_0 = 90^\circ$ point is shifted away from the aft axis out of the range of interest for the final solution. For inlet radiation, the $\psi_0 = 90^\circ$ point is shifted toward the inlet axis directly into the region of

interest for the solution. This will become evident in later sections and suggests that some improvements are required in the simplified inlet radiation equation.

Multimodal Inlet Radiation Directivity with Duct Flow

The simplified expressions for multimodal far-field radiation for an inlet with flow in the duct and no-flow in the surrounding medium will be presented here. The use of these equations will be discussed but sample calculations will be deferred to a later section.

The multimodal radiation pattern is given by

$$P_m^2(\psi) = \int_{\xi_D=1}^{\infty} F(\xi_D)\mathcal{D}(\xi_D)T(\xi_D)P_E^2(\psi,\xi_D)d\xi_D + B_s T(\xi_s)P_E^2(\psi,\xi_s) \qquad (27)$$

The first term represents the integration (or summation) of all of the randomly generated modes such as might occur in broadband noise or even for tones in a static engine test if inflow distortion is present. Notice that this term represents a continuum of modes and the actual number of modes is irrelevant as long as they are numerous. All of the equations in this paper have been derived in this way so that modal identity is unnecessary and only cut-off ratio is retained. The second term allows for a single discrete mode such as might be generated in an inlet at slightly supersonic rotor tip speeds. Since this mode would be uncorrelated with the randomly generated modes the pressures-squared can be added in this manner. Equation (27) could be extended to include additional discrete modes, but since they would probably be correlated, modal phasing would have to be considered and the pressures would have to be added before they are squared. Experimental data would have to be obtained very accurately and with fine angular resolution to make use of such a refined expression.

The term P_E^2 is the equal power per mode radiation expression given by Eq. (24), T is the duct termination loss coefficient given by Eq. (19), and $\mathscr{D}$ is the modal density function[6] given by,

$$\mathscr{D}(\xi_D) = \frac{2}{\xi_D^3} \tag{28}$$

which describes the relative density of the modes. The modal biasing function F and the modal amplitude B_s must be considered inputs from a noise source analysis or else derived from experimental radiation data. Saule,[45] Rice,[7], and Heidelberg, et al.,[49] have all attempted to infer source power distribution information from far-field radiation data, the latter two inferring the exponent n on a simple modal biasing function $F(\xi_o) = 1/\xi_o^n$ using a simple radiation expression based upon zero flow radiation theory ($P_m^2 \approx \cos \psi_o / \sin^n \psi_o$ from Ref. 7). Heidmann, et al.[29] and McArdle, et al.[50] have confirmed the presence of a single mode (essentially determining B_s in Eq. (27)) in inlet tests of an engine specially configured to produce the mode. They used the same angle transformations presented here to correct for the convective effects of duct flow and obtained good agreement between theory and data.

The simplist case for $F(\xi_D)$ is to consider it as a constant and let $B_s = 0$ in Eq. (27) and then the radiation directivity for equal energy per mode is represented. A more general expression can be formed by extending the modal biasing function presented by Rice[7] as a series in cut-off ratio given by

$$F(\xi_D) = \sum_{i=1}^{L} A_i \xi_D^{1-i} \tag{29}$$

The coefficients can be determined by forming the error relation,

$$E = \int_{\psi=0}^{\psi_{max}} \left[P_{ex}^2(\psi) - P_m^2(\psi)\right]^2 \sin\psi \, d\psi \tag{30}$$

and E can be minimized with respect to each unknown A_i and B_s to generate a system of equations for these unknowns. $P_{ex}^2(\psi)$ in Eq. (30) is the experimental data for the hardwalled inlet.

A theoretical attenuated far-field radiation directivity can be generated by using the attenuation function $\Delta dB(\xi_D)$ discussed in the suppressor section. This can be expressed as

$$P_{ma}^2(\psi) = \int_{\xi_D=1}^{\infty} 10^{[\Delta dB(\xi_D)/10]} F(\xi_D)\mathscr{D}(\xi_D)T(\xi_D)P_E^2(\psi,\xi_D)d\xi_D$$

$$+ B_s 10^{[\Delta dB(\xi_S)/10]} T(\xi_S)P_E^2(\psi,\xi_S) \tag{31}$$

The far-field attenuation directivity can then be given as

$$\Delta dB(\psi) = 10 \, \mathrm{Log}\left[\frac{P_{ma}^2(\psi)}{P_m^2(\psi)}\right] \tag{32}$$

At this time the integrals in Eqs. (27) and (31) are performed numerically. The modal density function has been used to select increments in ξ_D that contain equal numbers of modes. One hundred steps are used for the results to be shown later. Rice[7] has used an approximate integration scheme to produce a simple multimodal radiation equation for no flow. A comparable result for inlet radiation with duct flow is under development.

SAMPLE CALCULATIONS AND COMPARISON WITH EXPERIMENT

Several sample calculations will now be presented to show the character of the refinements made in the radiation equation to account for the convective effects of inlet duct flow. These calculations will be made for single

modes, multiple modes, and to demonstrate the determination of the modal biasing function from far-field radiation data.

Single Modes

The radiation directivities for two modes are shown in Fig. 5 for no flow and in Fig. 6 for $M_D = -0.221$. Note that the ordinate is the directivity weighted by the modal density function and the duct termination loss as occurs in the integrand of Eqs. (27) and (31). Several modes could have been selected in Fig. 5 which would have shown good comparisons with Wiener-Hopf solutions. However these two modes, or more accurately these two cutoff ratios, were selected to show a problem with the radiation model which needs correction. In Fig. 5 both modes are represented withsufficient accuracy up to $\psi = 90^\circ$. However beyond $\psi = 90^\circ$ note that for $\xi_0 = 1.05$ the directivity curve experiences a mild second peak with a rapid rolloff at higher angles. According to Homicz and Lordi[15] when a peak occurs beyond $\psi = 90^\circ$ in the Wiener-Hopf solution a single broad lobe occurs with no zeroes. This aft lobe in Fig. 5 thus cannot be considered accurate. The second mode, for $\xi_0 = 1.1261$, was chosen to produce a minimum at $\psi = 90^\circ$. An inspection of the results of Candel[20] seems to indicate that when a lobe minimizes at $\psi = 90^\circ$ there is essentially no radiation at all in the aft quadrant for an unflanged duct. The present solution produces a lobe peaking at $\psi = 115^\circ$ which must be considered completely spurious. Again it should be emphasized that the radiation directivities in Fig. 5 are perfectly adequate up to $\psi = 90^\circ$. However when $M_D = -0.221$ as in Fig. 6, both radiation directivities are shifted toward the inlet axis. Now the questionable peak for $\xi_D = 1.05$ dominates the radiation at $\psi = 90^\circ$ and the spurious aft lobe for $\xi_D = 1.1261$ is beginning to contribute (a larger inlet Mach number would cause it to dominate). It is thus obvious

that with an inlet duct flow the present model will overpredict the true radiation pattern at angles near the sideline.

It should be expected that when an analysis is pushed beyond its range of validity, some errors will result. In this case it was necessary since no exact solutions exist to handle the flow conditions of a realistic inlet. Alterations to the theory will be pursued to insure more realistic representation of the broad lobe in the aft quadrant and to remove spurious aft lobes.

Multimodal Radiation Directivity

Several multimodal radiation directivities are shown in Fig. 7 for equal acoustic power per mode and duct Mach numbers ranging from $M_D = 0$ to -0.8. These calculations were made using Eq. (27) with $B_s = 0$ and also Eq. (29) with $A_1 = 10^7$ and all other $A_i = 0$. For $M_D = 0$, the curve in Fig. 7 reproduces previously published[7,46] results but with improved accuracy between $\psi = 80^\circ$ to 90°. As inlet Mach number is introduced, the radiation directivity is shifted dramatically toward the inlet axis. At $M_D = -0.8$ most of the radiation is confined to the front 30°. The reversal or oscillations in the directivities at larger angles are caused by inadequately represented aft lobes discussed in the previous section. The directivities should show a monotonic fall-off at large angles and the portion of the curves with oscillations are not considered valid.

Determination of Modal Biasing Function

Inlet radiation data from Ref. 49 for the blade passage frequency from a Lycoming YF102 engine at approach engine speed are shown in Fig. 8. A massive aft suppressor was used so that the data can be considered to originate from the inlet. Equation (27) was used for the theoretical radiation curves with the extra discrete mode amplitude, $B_s = 0$. The modal biasing

function ($F(\xi_D)$ from Eq. (29)) was allowed to contain one to three coefficients. With one coefficient equal acoustic power per mode is assumed. It is seen from Fig. 8 that the data indicates that more power is present at low cut-off ratios (larger angles) than equal power per mode allows. When two or three coefficients are allowed the dashed curve of Fig. 8 is obtained. This provides a better fit to the data but the upturn in the theoretical curve beyond 80° shows the effect of the spurious aft lobes. Much more experimentation is required into the best form of the modal biasing function.

Suppressor Calculations

The experimental radiation directivity attenuation (from same data as Fig. 8) at blade passage frequency for liner B3 (see Ref. 49) is shown in Fig. 8. The theoretical suppression directivities were generated using Eqs. (27), (31), and (32) with three coefficients used in the modal biasing function of Eq. (29). A series of liner resistances were used to generate the theoretical curves in Fig. 9. Notice that for liner resistances in the range of about 1.5 to 5 (resistance normalized by ρc) the theory agrees quite well with the data. Also recall that for angles greater than about 80° the theory as presently formulated cannot be trusted due to the spurious aft lobes. The liner resistance, as calculated from the impedance model for perforated plate (see Ref. 49), is 0.875. This value has not been corrected for potential hole blockage which may increase the resistance to possibly 1.1 (20 percent blockage). Even with this correction the theory must be considered as underpredicting this data. The theory is qualitatively correct in predicting larger attenuation near the sideline and low attenuation near the inlet axis. The theory is also qualitatively similar to that of Kempton[37,38] who used ray acoustics with no-flow.

The suppressor directivity theory was used to predict the loss of suppressor effectiveness with increasing suppressor length as shown in Fig. 10. This loss of suppressor performance is inherent in the complex structure of the radiation pattern. For short suppressors the principal lobes of the easily attenuated modes near cut-off show large reductions near the sideline. As suppressor length is increased the sidelobes of the higher cut-off ratio modes limit the suppression at the near sideline angles and additional suppression can be otained only by reducing these more difficult to suppress modes. Suppressor effectiveness is thus progressively reduced as more length is added. The angle of peak attenuation is also shown to move toward angles nearer the inlet axis. Another phenomenon exists to produce this same result but it is not as yet included in the present model. As a mode enters the suppressor it is scattered into higher radial orders which may damp quite easily. As suppressor length increases only the least attenuated mode remains and $\Delta dB/L/D$ will flatten out when plotted against L/D. This effect has not as yet been proven to be a dominant factor for multimodal excitation of the liner.

CONCLUDING REMARKS

The method of suppressor analysis based upon mode cut-off ratio has been reviewed here. The technique appears to be a viable method of analysis of the entire inlet suppressor system including provisions for noise source characteristics, sound propagation through acoustically lined ducts, duct termination effects, and radiation to the far-field. The key to the method for use with many modes is that individual modal identification is not required but is instead represented through the mode cut-off ratio. The modes are considered to be distributed in a continuum of cut-off ratios and the possibility that large numbers of modes may be present (high frequency

broadband noise) poses no problem. For single or only a few modes, classical modal analysis is suggested, but some of the angle transformations given here must be used to obtain reasonable far-field radiation results for realistic inlet flow conditions.

The new contributions to the method presented here are the inclusion of the effect of inlet duct flow (far-field static) on the radiation directivity, an improved method of evaluating the source modal biasing function (source power distribution), and the removal of the pressure doubling effect of the flange of the simple radiation model used here. Several interesting phenomena have been demonstrated by exercising the present model. The far-field directivity attenuation can be shown to peak near the angles suggested by experimental data. For a constant source sound power distribution, increased duct Mach number causes the radiation to be moved toward the inlet axis. The radiation directivity has been shown to be a strong function of source power distribution. Although not shown here, preliminary calculations have shown that radiation directivity attenuation is only a weak function of source power distribution (for many modes) agreeing with the results of Kempton.[37,38] The loss of suppressor efficiency with increasing length has been shown to be an inherent property of a multimodal source.

Several improvements must be made to achieve quantitative agreement with experimental data. The method provides for the convenient inclusion of improved physics due to its modular nature which also allows for selective empiricism to be incorporated if required. Modal scattering in the acoustic liner must be studied, correlated, and incorporated into the program if it is significant. The effects of duct area variation and flow gradients must be considered. The modification of the radiation pattern by inlet lip shape and refraction through accelerated flows near the lip must be studied. Of

most immediate concern is the removal of the spurious aft lobes in the flanged duct radiation equation which are shifted into the forward quadrant due to duct flow convection effects. The biggest problem is that there is no exact solution with which comparisons can be made. Kinematic corrections must be made to the Wiener-Hopf solutions to simulate solutions for realistic inlet flows and there is no guarantee that the diffraction effects are properly modeled. Two approaches might be tried. The Wiener-Hopf solution for uniform flow everywhere must undergo an angle transformation to remove the effect of the far-field flow (which must be static). The second approach might be to use the Wiener-Hopf solution with a tube of flow extending from the inlet (static surrounding medium) and then remove the effect of refraction through the rotational flow slip layer that does not actually exist in a real inlet flow. The first approach has shown promising results for matching a single mode principal lobe to experimental data in an engine inlet test.[50] The second approach was used in reverse order for an aft radiation problem where the Wiener-Hopf solution is valid. The flanged duct model was transformed to account for convection and refraction[30] and agreed well with the Wiener-Hopf solution.

REFERENCES

1. A. H. Nayfeh, J. E. Kaiser, and D. P. Telionis, "Acoustics of Aircraft Engine-Duct Systems," AIAA J., 13, 130-153 (1975).
2. P. G. Vaidya and P. D. Dean, "State of the Art of Duct Acoustics," AIAA Paper No. 77-1279 (Oct. 1977).
3. A. A. Syed and S. C. Bennett, "Comparison of Measured Broadband Noise Attenuation Spectra from Circular Flow Ducts and from Lined Engine Intakes with Predictions," J. Sound Vib., 56, 531-564 (1978).

4. E. J. Rice, "Acoustic Liner Optimum Impedance for Spinning Modes with Mode Cut-off Ratio as the Design Criterion," AIAA Paper No. 76-516 (July 1976); also NASA TM X-73411 (1976).

5. E. J. Rice, "Inlet Noise Suppressor Design Method Based upon the Distribution of Acoustic Power with Mode Cutoff Ratio," Advances in Engineering Science, NASA CP-2001, Vol. 3 (1976), pp. 883-894.

6. E. J. Rice, "Modal Density Function and Number of Propagating Modes in Ducts," NASA TM X-73539 (1976).

7. E. J. Rice, "Multimodal Far-Field Acoustic Radiation Pattern Using Mode Cutoff Ratio," AIAA J., 16, 906-911 (1978).

8. E. J. Rice and L. J. Heidelberg, "Comparison of Inlet Suppressor Data with Approximate Theory Based on Cut-off Ratio," Journal of Aircraft (to be published), also AIAA Paper No. 80-0100 (Jan. 1980) and NASA TM-81386 (1980).

9. J. M. Tyler and T. G. Sofrin, "Axial Flow Compressor Noise Studies," SAE Trans., 70, 309-332 (1962).

10. H. Levine and J. Schwinger, "On the Radiation of Sound from an Unflanged Circular Pipe," Phys. Rev., 73, 383-406 (1948).

11. G. F. Carrier, "Sound Transmission from a Tube with Flow," Q. Appl. Math., 13, 457-461 (1955-1956).

12. L. A. Weinstein (Vainshtein), The Theory of Diffraction and Factorization Method (The Golem Press, Boulder, CO, 1969).

13. D. L. Lansing, "Exact Solution for Radiation of Sound from a Semi-Infinite Circular Duct with Application to Fan and Compressor Noise," Analytical Methods in Aircraft Aerodynamics, NASA SP-228 (1969), pp. 323-334.

14. D. L. Lansing, J. A. Drischler, and C. G. Pusey, "Radiation of Sound from an Unflanged Circular Duct with Flow," Acoustical Society 79th. Spring Meeting, Atlantic City, NJ (April 21-24, 1970) Session D, Paper 5.

15. G. F. Homicz and J. A. Lordi, "A Note on the Radiative Directivity Patterns of Duct Acoustic Modes," J. Sound Vib., 41, 283-290 (1975).

16. S. D. Savkar and I. H. Edelfelt, "Radiation of Cylindrical Duct Acoustic Modes with Flow Mismatch," Report SRD-75-029, General Electric Co., Schenectady, NY (March 1975). Also NASA CR-132613 (1975).

17. S. D. Savkar, "Radiation of Cylindrical Duct Acoustic Modes with Flow Mismatch," J. Sound Vib., 42, 363-386 (1975).

18. R. M. Munt, "The Interaction of Sound with a Subsonic Jet Issuing from a Semi-Infinite Cylindrical Pipe," J. Fluid Mech., 83, 609-640 (1977).

19. S. W. Rienstra, "On the Acoustical Implications of Vortex Shedding from an Exhaust Pipe," Presented at the ASME 1980 Winter Annual Meeting (Nov. 16-21, 1980), Chicago, IL. Also ASME Paper No. 80-WA/NC-16 (Nov. 1980).

20. S. M. Candel, "Acoustic Radiation from the End of a Two-Dimensional Duct; Effects of Uniform Flow and Duct Lining," J. Sound Vib., 28, 1-13 (1973).

21. W. Koch, "Radiation of Sound from a Two-Dimensional Acoustically Lined Duct," J. Sound Vib, 55, 255-274 (1977).

22. P. Mungur, H. E. Plumblee, and P. E. Doak, "Analysis of Acoustic Radiation in a Jet Flow Environment," J. Sound Vib., 36, 21-52 (1974).

23. P. Mungur and H. E. Plumblee, "Influence of a Jet Exhaust Flow Field on the Acoustic Radiation Impedance of a Jet Pipe Opening," AIAA Paper No. 79-0676 (Mar. 1979).

24. H. E. Plumblee, "Radiation of Duct Noise Out Through a Jet Flow," AIAA Paper No. 75-457 (Mar. 1975).

25. J. L. Whitesides and P. Mungur, "On the Influence of Temperature Gradients in Jet Flows on the Radiation of Sound," 86th Meeting, Acoustical Society of American (Oct. 30 - Nov. 2, 1973), Los Angeles, CA, Session H, Paper H11.

26. R. J. Beckemeyer, D. T. Sawdy and P. Garner, "Computational Methods for Acoustic Radiation from Circular Ducts," in Aeroacoustics: Fan Noise and Control; Duct Acoustics; Rotor Noise, edited by I. R. Schwartz, H. T. Nagamatsu, and W. C. Straehle, AIAA Progress in Astronautics and Aeronautics, Vol. 44 (American Institute of Aeronautics and Astronautics, New York, 1976), pp. 415-432.

27. D. T. Sawdy, R. J. Beckemeyer and P. Garner, "Effects of a Conical Segment on Sound Radiation from a Circular Duct," in Aeroacoustics: Fan Noise and Controls; Duct Acoustics; Rotor Noise, edited by I. R. Schwartz, H. T. Nagamatsu, and W. C. Straehle, AIAA Progress in Astronautics and Aeronautics, 44 (American Institute of Aeronautics and Astronautics, New York, 1976), pp. 433-450.

28. E. J. Rice, M. F. Heidmann, and T. G. Sofrin, "Modal Propagation Angles in a Cylindrical Duct with Flow and Their Relation to Sound Radiation," AIAA Paper No. 79-0183 (Jan. 1979). Also NASA TM-79030 (1978).

29. M. F. Heidmann, A. V. Saule and J. G. McArdle, "Predicted and Observed Modal Radiation Patterns from JT15D Engine with Inlet Rods," J. Aircraft, 17, 493-499 (1980).

30. E. J. Rice and A. V. Saule, "Far-Field Radiation of Aft Turbofan Noise," NASA TM-81506 (1980).

31. W. E. Zorumski, "Generalized Radiation Impedance and Reflection Coefficients of Circular and Annual Ducts," J. Acoust. Soc., Am., 54, 1667-1673 (1973).

32. R. E. Motsinger, R. E. Kraft, and J. W. Zwick, "Design of Optimum Acoustic Treatment for Rectangular Ducts with Flow," ASME Paper No. 76 GT-113 (Mar. 1976).

33. G. L. Minner, and E. J. Rice, "Computer Method for Design of Acoustic Liners for Turbofan Engines," NASA TM X-3317 (1976).

34. E. J. Rice, "Spinning Mode Sound Propagation in Ducts with Acoustic Treatment," NASA TN D-7913 (1975).

35. S. H. Ko, "Sound Attenuation in Acoustically Lined Circular Ducts in the Presence of Uniform Flow and Shear Flow," J. Sound Vib., 22, 193-210 (1972).

36. K. J. Baumeister, "Numerical Techniques in Linear Duct Acoustics." NASA TM-81553 (1980).

37. A. J. Kempton, "A Ray-Theory Approach for High-Frequency Engine-Intake Noise," Proceedings of the Joint Symposium on Mechanics of Sound Generation in Flows, edited by E. A. Muller (Springer-Verlag, New York, 1979), pp. 203-209.

38. A. J. Kempton, "Ray Theory to Predict the Propagation of Broadband Fan-Noise," AIAA Paper No. 80-0968 (June 1980).

39. E. J. Rice, "Modal Propagation Angles in Ducts with Soft Walls and Their Connection with Suppressor Performance," AIAA Paper No. 79-0624 (Mar. 1979); also NASA TM-79081 (1979).

40. Y. C. Cho and E. J. Rice, "High-Frequency Sound Propagation in a Spatially Varying Mean Flow," NASA TM-81751 (1980).

41. T. G. Sofrin and J. F. McCann, "Pratt and Whitney Experience in Compressor-Noise Reduction," abstracted in Journal of the Acoustical Society of America, 40, 1248-1249 (1966). Also Presented at 72nd Meeting of the Acoustical Society of America, Los Angeles, CA (Nov. 1966), Session 2D, Paper 2D2.

42. E. J. Rice, "Optimum Wall Impedance for Spinning Modes - a Correlation with Mode Cutoff Ratio," J. Aircraft, 16, 336-343 (1979).

43. E. J. Rice, "Spinning Mode Sound Propagation in Ducts with Acoustic Treatment and Sheared Flow," in Aeroacoustics: Fan Noise and Control; Duct Acoustics; Rotor Noise, edited by I. R. Schwartz, H. T. Nagamasu, and W. C. Straehle, AIAA Progress in Astronautics and Aeronautics, Vol. 44 (American Institute of Aeronautical and Astronautics, New York, 1976), pp. 475-505. Also AIAA Paper No. 74-519 (Mar. 1975) and NASA TM X-71672 (1975).

44. E. J. Rice, "Attenuation of Sound in Ducts with Acoustic Treatment: A Generalized Approximate Equation," NASA TM X-71830 (1975).

45. A. V. Saule, "Modal Structure Inferred from Static Far-Field Noise Directivity," AIAA Paper No. 76-574 (July 1976). Also NASA TM X-71909 (1976).

46. A. V. Saule and E. J. Rice, "Far-Field Multimodal Acoustic Radiation Directivity," NASA TM-73839 (1977).

47. Y. C. Cho and K. U. Ingard, "Higher Order Mode Propagation in Nonuniform Circular Ducts," AIAA Paper No. 80-1018 (June 1980). Also NASA TM-81481 (1980).

48. J. W. Posey, L. R. Clark and R. J. Silcox, "Angles of Peak Sound Radiation from Axisymmetric Duct Inlets," Presented at the 100th meeting of the Acoustical Society of America, Los Angeles, CA (Nov. 1980), Session VV, Paper VV8.

49. L. J. Heidelberg, E. J. Rice, and L. Homyak, "Experimental Evaluation of a Spinning Mode Acoustic-Treatment Design Concept for Aircraft Inlets," NASA TP-1613 (1980).

50. J. G. McArdle, W. L. Jones, L. J. Heidelberg and L. Homyak, "Comparison of Several Inflow Control Devices for Flight Simulation of Fan Tone Noise Using a JT15D-1 Engine," AIAA Paper No. 80-1025 (June 1980).

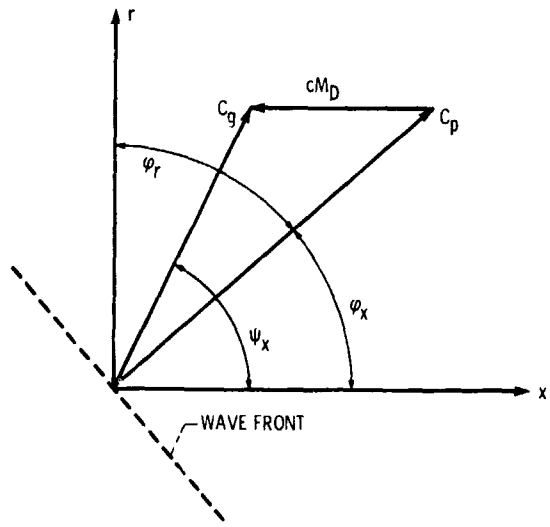

Figure 1. - Propagation angles with duct flow.

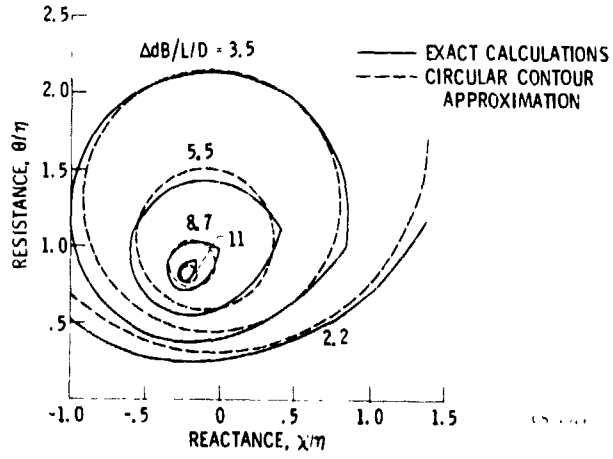

Figure 2. - Comparison of exact and approximate equal damping contours for a well propagating mode. $m = 7$, $\mu = 1$, $\eta = 10$, $M_D = -0.4$, $\varepsilon = 0.002$.

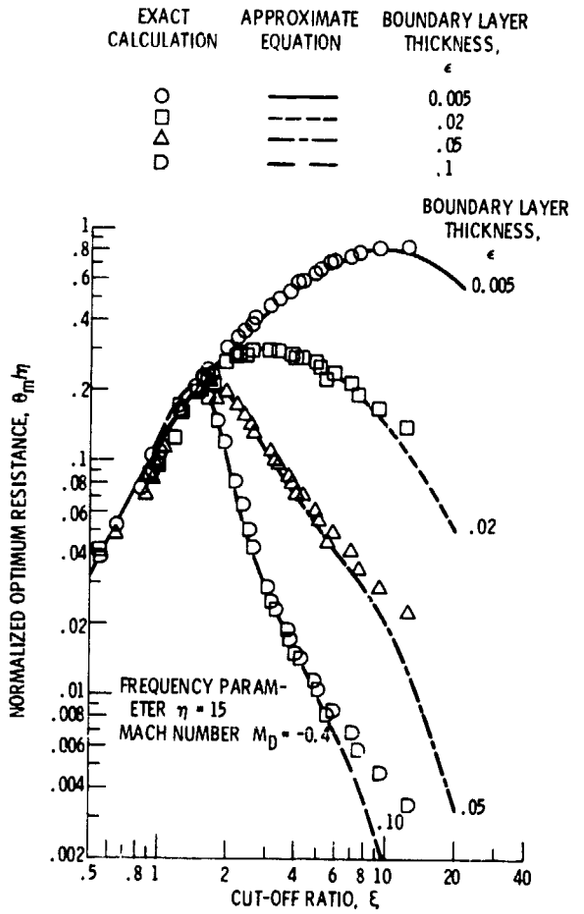

Figure 3. - Comparison of correlating equation with exact calculations of optimum resistance for variations in boundary layer thickness.

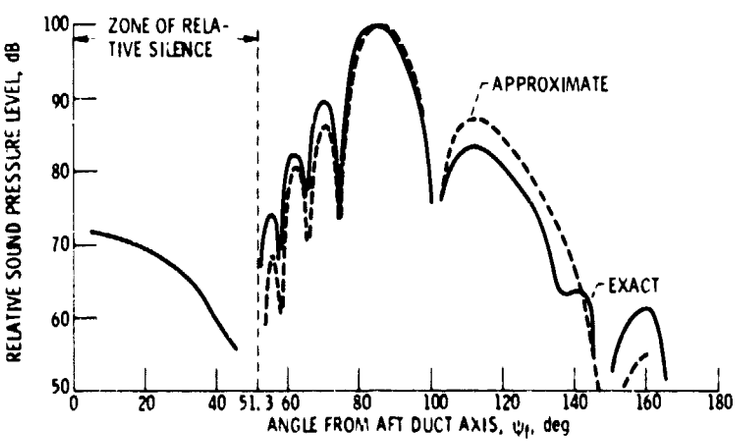

Figure 4. - Comparison of approximate and exact aft radiation patterns for mode (8,4); M_D = 0.6; M_f = 0; η = 7.11.

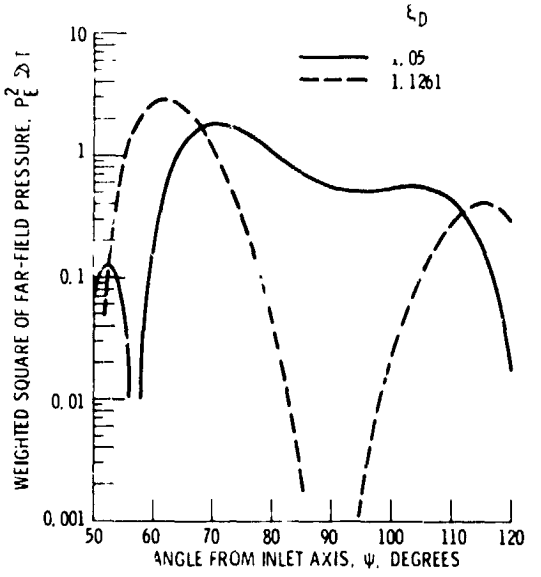

Figure 5 - Far-field radiation directivity for two modes $\eta = 8.93$, $M_D = 0$.

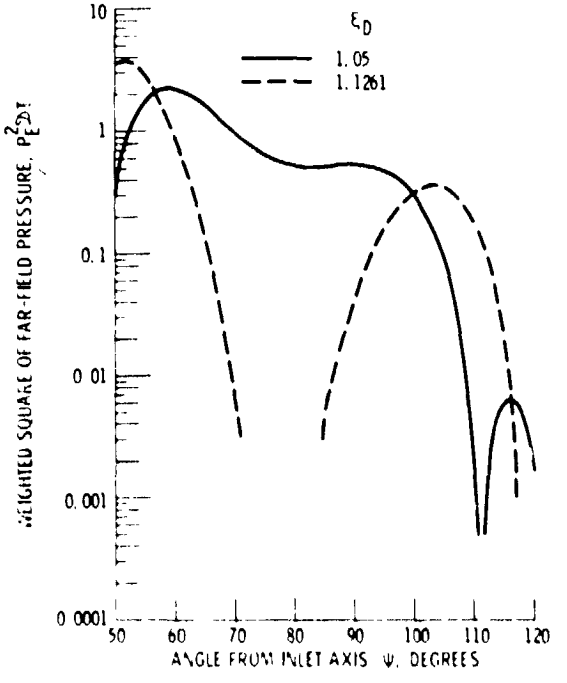

Figure 6 - Far-field radiation directivity for two modes $\eta = 8.93$ $M_D = -0.221$

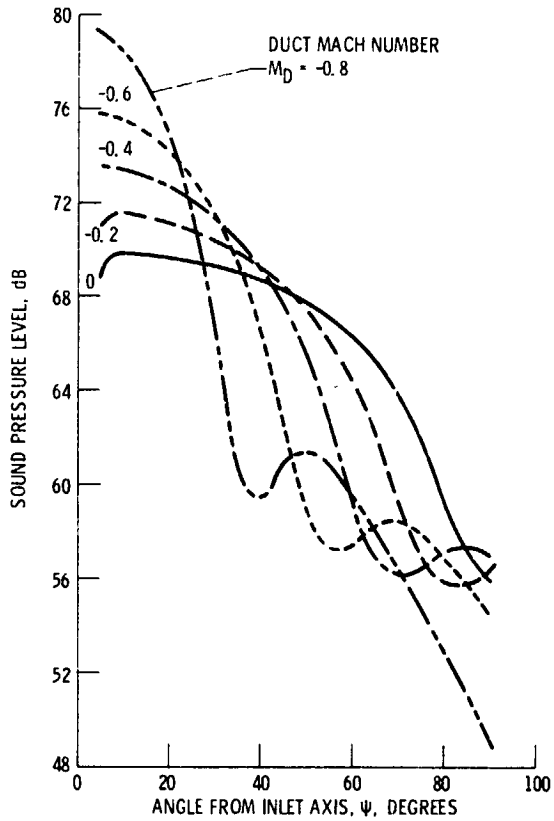

Figure 7. - Far-field radiation directivity for equal acoustic power per mode, $\eta = 14.09$.

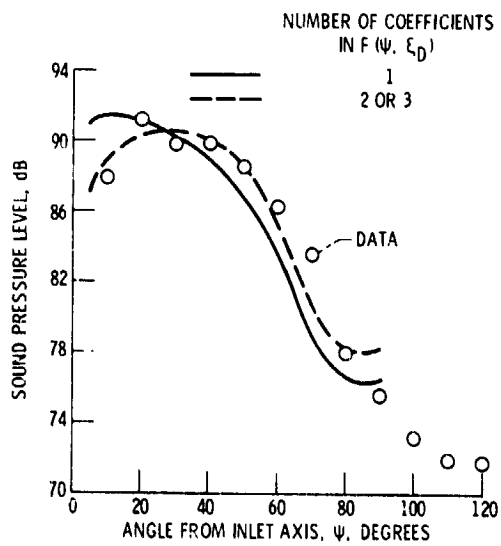

Figure 8. - Example of fitting radiation theory to experimental data by varying model biasing function, $F(\psi, \xi_D)$, $\eta = 8.93$, $M_D = -0.221$, data from reference 49.

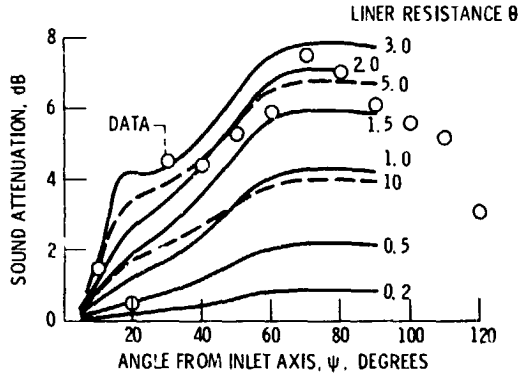

Figure 9. - Comparison of theoretical and experimental far-field directivity attenuations, data reference 49, blade passage frequency, $\eta = 8.93$, $M_D = 0.221$, $\chi = -2.652$, $\varepsilon = 0.071$, L/D = 1/2.

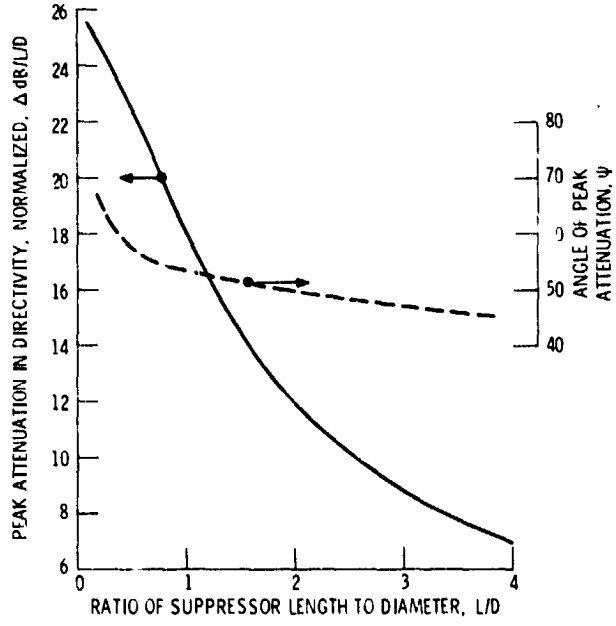

Figure 10. - Theoretical loss of suppressor efficiency with increasing length, $\eta = 14.09$, $M_D = -0.375$, $\varepsilon = 0.071$, $\theta = 1.171$, $\chi = -1.171$